Table 1

	Values of v_θ						Values of v_r				
ρ	$\theta = 90°$	$\theta = 92.5°$	$\theta = 95°$	$\theta = 100°$	$\theta = 120°$	$\theta = 180°$	$\theta = 90°$	$\theta = 95°$	$\theta = 100°$	$\theta = 120°$	$\theta = 180°$
1.0	0	0	0	0	0	0	0.56419	0.56419	0.56419	0.56419	0.56419
1.01	0.09562	0.08240	0.07141	0.05238	0.01869	0	0.64339	0.64348	...	...	0.64354
1.04	0.26532	0.23165	0.20012	0.14678	0.05201	0	0.71916	0.71965	...	...	0.72000
1.06	0.34714	0.30448	0.26365	0.19339	0.06821	0	0.75131	0.75208	...	...	0.75262
1.08	0.41497	0.36569	0.31741	0.23284	0.08176	0	0.77729	0.77831	...	...	0.77903
1.10	0.47254	0.41841	0.36406	0.26706	0.09336	0	0.79923	0.80049	0.80110	0.80137	0.80137
1.20	0.66518	0.60347	0.53166	0.38971	0.13344	0	0.87606	0.87826	0.87930	0.87970	0.87970
1.5	0.85138	0.83190	0.76002	0.54871	0.17866	0	0.98471	0.98808	0.98961	0.98994	0.98994
2.0	0.82976	0.91637	0.87908	0.59393	0.18470	0	1.05279	1.05668	1.05755	1.05764	1.05764
3.0	0.66075	0.92772	0.90951	0.51801	0.15828	0	1.09611	1.09888	1.09929	...	1.09930
4.2	0.51094	0.94586	0.82421	0.42097	0.12857	0	1.11215	1.11408	1.11414	...	1.11414
5.0	0.44154	0.96712	0.74354	0.37165	0.11351	0	1.11699	1.11848	1.11849	...	1.11849
7.0	0.32808	0.98817	0.57581	0.28572	0.08726	0	1.12259	1.12346	...	...	1.12346
10.0	0.23604	0.84005	0.42575	0.21124	0.06452	0	1.12555	1.12601	...	...	1.12601

velocity, the gas flowing out directly at the surface, a Maxwellian distribution. A true Maxwellian distribution is isotropic and yields no net outward flux; rather, a Maxwellian distribution times the step function $S = 1$ for directions out of the surface and $S = 0$ for directions into the surface is appropriate. However, the normalization of such a distribution must be twice that of a Maxwellian distribution in order for the integral over all directions to equal the local number density. This factor of 2 in the normalization was not used in deriving the approximate boundary condition and hence not used in deriving Eq. (2). If it had been, the right-hand side of Eq. (2) would have been half as big.

The further differences between Eqs. (2) and (4) enter from approximations to the flux equality condition which were made in deriving the boundary condition for Eq. (2), essentially ignoring the dependance of the mathematical expression with position on the surface. The approximation to the Wang Chang distribution used to derive Eq. (3) amounted to using a more accurate approximation to the flux equality condition.

The mean velocity $\bar{v}$ of the reflected particles at any point can be found by averaging $\bar{v}$ using the Wang Chang distribution function. Using the same approximation to the distribution function, closed-form analytic results for the tangential and radial components v_θ and v_r are, respectively,

$$v_\theta = (V/Sn)\ \mathrm{erfc}(V\rho\cos\theta)\ \sin\theta F_1(\rho)$$

where

$$F_1(\rho) = \frac{1}{\rho^3} - \left(1 + \frac{P^2}{2}\right) + P^2\rho\left(1 - \frac{P^2}{4}\right)\log_e\left(\frac{\rho+1}{\rho-1}\right) \tag{5}$$

and

$$v_r = [2(\pi)^{1/2}n]^{-1}\{\rho^{-2}\exp[-(V\cos\theta)^2] - \tfrac{1}{2}(\pi)^{1/2}V\cos\theta F_2(\rho)\ \mathrm{erfc}(V\rho\cos\theta)\}$$

where

$$F_2(\rho) = \frac{1}{\rho^3} + 1 - \frac{P^2}{2} - \frac{P^4\rho}{4}\log_e\left(\frac{\rho+1}{\rho-1}\right)$$

and

$$P = (1 - \rho^{-2})^{1/2}$$

The details of these integrations are given in Appendix B of Ref. 5, whereas numerical results for $V = 5$ are given here in Table 1. They indicate insensitivity of v_r to angle and in general indicate a monotone build-up of radial velocity with radial distance. Tangential velocity as a function of ρ builds up as would be expected from zero and then drops off. Further v_θ changes rapidly with decreasing θ near $\theta = 90°$, the radial position of the maximum dropping rapidly.

References

[1] Gurevich, A. V., "Perturbations in the ionosphere caused by a traveling body," *Artificial Earth Satellites* (Iskusstvennye Sputniki Zemli) **7**, 101–124 (1961); transl. by R. Matthews in Planetary Space Sci. **9**, 321–344 (1962).

[2] Probstein, R. F., "Shock wave and flow field development in hypersonic re-entry," ARS J. **31**, 185–194 (1961).

[3] Dolph, C. L. and Weil, H., "On the change in radar cross section of a spherical satellite caused by a plasma sheath," *Electromagnetic Effects of Re-entry* (Pergamon Press, London, 1961); reprinted in Planetary Space Sci. **6**, 123–132 (1961).

[4] Wang Chang, C. S., "Transport phenomena in very dilute gases, II," Univ. Mich. Eng. Research Inst. Rept. CM-654 (December 1950).

[5] Weil, H. and Barasch, M. L., "A theoretical lunar ionosphere," Icarus **1**, 346–356 (1963).

Interactions between a Hypersonic Wake and a Following Hypersonic Projectile

R. E. Slattery,* W. G. Clay,† and R. R. Stevens‡

Lincoln Laboratory,§ Massachusetts Institute of Technology, Lexington, Mass.

During a recent series of experiments at the Lincoln Laboratory Re-entry Simulating Range, it was discovered that the presence of the sabot in the wake of a spin-stabilized cone radically altered the flow around the cone. The base section of the sabot is partially split, so that normally it breaks upon leaving the gun muzzle, and the pieces are separated from the cone's flight path by centrifugal forces. When the sabot base fails to split, as sometimes occurs, it continues downrange along the same path as the cone, slowly falling behind it because of the differences in drag.

In Fig. 1 is shown a schlieren photograph of a 25° included-angle cone in normal, zero attitude flight at 5500 fps through 25 mm Hg of dry air. The techniques of stabilized flight,

Received January 3, 1963.

* Assistant Leader, Plasma Physics Group.

† Staff Member, Plasma Physics Group.

‡ Project Technician, Plasma Physics Group.

§ Operated with support from the U. S. Advanced Research Projects Agency.

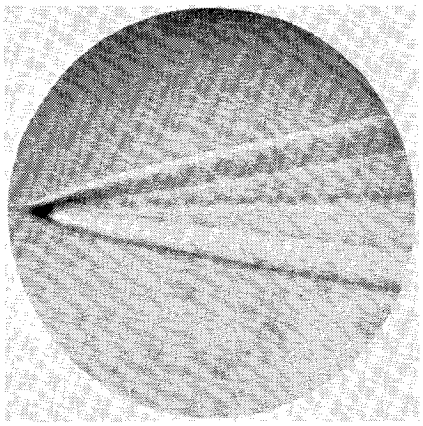

Fig. 1 25° included angle cone in normal flight (5500 fps, 25 mm Hg air pressure)

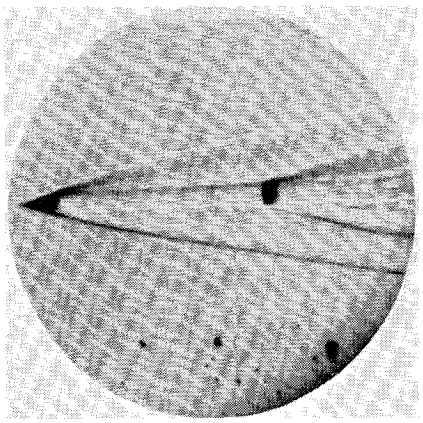

Fig. 2 25° included angle cone followed by a piece of sabot (5500 fps, 25 mm Hg air pressure)

schlieren photography, and assurance of constant attitude have been described elsewhere.[1] Note that the characteristics of the flow are as expected. There are bow and secondary shocks, and the laminar trail is much narrower than the base of the cone. There is a distinct necking of the flow, causing the secondary shock, and, further downstream, there is a distinct laminar-to-turbulent transition. Hundreds of pictures like this have been taken under various flight conditions.

Figure 2 shows an identical cone fired under precisely the same conditions, but with the base of the sabot located in the wake of the cone and some distance behind it. Note that the flow behind the cone is completely different in this case. There is no secondary shock. There is no necking of the flow. The trail is still laminar but of approximately the diameter of the base. No hint of laminar to turbulent transition exists ahead of the sabot. Examination of the film density of the schlieren photograph indicates that, as in Fig. 1, the laminar trail is a region of much lower gas density than the surrounding inviscid region (an expected temperature and pressure phenomenon in the case of the normal flow this close to the body). Obviously, the cone and sabot have interacted via the wake of the cone. This is *not* an isolated phenomenon; the results are completely reproducible.

The first and obvious lesson from these two photographs is that considerable care must be taken by researchers in ballistic ranges to insure that sabots separate properly and that the field of view of their optics is sufficiently wide so that the possibility of the interaction between two or more projectiles is eliminated. Otherwise, the flow characteristics photographed are not necessarily those of the body under study.

[1] Slattery, R. E. and Clay, W. G., "The turbulent wake of hypersonic bodies," ARS Preprint 2673-62 (1962).

Figure 2 is interesting in and for itself. The sabot, traveling in the wake of the cone, has made its presence felt upstream and has changed the otherwise normal flow about the cone. The simplest interpretation is that the sabot is immersed in a fluid with respect to which it has a *subsonic* velocity, despite its high velocity in the laboratory system. Under these conditions it can propagate energy back up the cone's trail, countercurrent to the flow in the trail (in the body-centered system), and alter the characteristic flow about the cone. This comes about, probably, for two reasons: 1) the flow in the wake of the cone is quite high speed in the observer system and is an appreciable fraction of the velocity of the sabot; and 2) the flow is hot, which tends to raise the sound speed.

Of course, having stated that energy is propagated up the trail by no means describes the details of the processes that alter the normal flow.

Invariant Components of Motion in Inverse-Square Force Fields

FREDERICK V. POHLE*
Adelphi College, Garden City, N. Y.

CRONIN and Schwartz[1] have drawn attention to a useful, but little known, property of motion in a two-body motion in an inverse-square force field, namely, that the velocity vector can be resolved at any point into two components of constant magnitude, one remaining normal to the initial line and the other remaining normal to the radius vector. This property of the motion also has been proved in the well-known text on dynamics by Whittaker.[2] The present note is a brief outline of work[3] published in 1959 which used the same invariant properties and applied the method to the problem of small drag and low thrust.

Kepler's second law states that the radius vector sweeps out equal areas in equal times; the quantity $r^2(d\vartheta/dt) = h$ is a constant of the motion and is, of course, a first integral of the equations of motion. Here ϑ is the true anomaly and h is a constant.

The existence of an invariant such as $r^2(d\vartheta/dt)$ immediately suggests the problem of finding additional invariants, and this search is successful if the invariant components just noted are used. If v_1 denotes the component normal to the initial line and v_2 denotes the component normal to the radius vector (V_p and V_h, respectively, in Fig. 2 of Ref. 1), then it also is of interest to note that v_1/v_2 is the eccentricity of the orbit. The square of the speed then is given by

$$v^2 = v_1^2 + v_2^2 + 2v_1v_2\cos(\vartheta)$$

If, further, a is the semimajor axis of the elliptical orbit, e the eccentricity of the orbit, and R the radius of the earth, the three invariants of the motion can be written as

$$\begin{aligned} x &= p(d\vartheta/dt) - (dp/dt)\cot(\vartheta) = (R/L)^{1/2} \\ y &= (dp/dt)/\sin(\vartheta) = e(R/L)^{1/2} \\ z &= p^2(d\vartheta/dt) = (L/R)^{1/2} \end{aligned} \qquad (1)$$

In Eqs. (1), $p = r/R$ and $L = a(1 - e^2)$; for convenience, the area integral is denoted by z, and v_1 and v_2 now are denoted by y and x, respectively. The quantities x and z are dependent in the classical case; in the following, x,y, and z will be used as new dependent variables, with ϑ as the new independent variable. The original dependent variables were r and ϑ as functions of the time t.

Received January 2, 1963. The work reported here originally was done when the author was Professor of Applied Mechanics at the Polytechnic Institute of Brooklyn, Brooklyn, N. Y.

* Professor of Mathematics. Associate Fellow Member AIAA.